博 士 論 文

Histochemical analysis of osteoclast and osteoblast distributions on a hydroxyapatite/collagen bone-like nanocomposite embedded in rat tibiae
（ラット脛骨に埋入したハイドロキシアパタイト コラーゲンナノ複合材における破骨細胞と骨芽細胞分布の組織化学的解析）

令和７年３月申請

北海道大学

大学院歯学院口腔医学専攻

榊　原　真　子

Abstract

Objective: To clarify how the orientation of hydroxyapatite and collagen bone-like nanocomposite (HAp/Col) fibers in a HAp/Col block affects bone resorption and formation, HAp/Col cylinders with laminated collagen layers were implanted into the tibial diaphysis of rats and examined histochemically.

Materials and Methods: HAp/Col fibers were synthesized by the simultaneous titration method to form HAp nanocrystals on collagen fibers similar to bone nanostructure. Cylindrical HAp/Col blocks were formed by uni-axially compressing to layer them with maintaining their consistent horizontal alignment. The cylindrical HAp/Col grafts were implanted into cortical bone cavities of 10-week-old male Wistar rats, ensuring that the HAp/Col fiber bundles were parallel to the tibial surface. The blocks were analyzed histologically 3, 5, 7, 14, and 28 days after implantation in two regions: the lateral side facing the cortical bone (perpendicular to the HAp/Col layers), and the bottom region (near the marrow, parallel to the collagen layers).

Results and Discussion: TRAP-positive osteoclasts were observed in the lateral region 3–5 days after implantation but rarely seen in the bottom region. By day 7, many TRAP-positive osteoclasts had accumulated only in the lateral region, while osteoclasts appeared in both regions by day 14. By day 28, many osteoclasts were present throughout the cylinder. PHOSPHO1-positive osteoblasts were first detected on day 5, located slightly away from the HAp/Col cylinder in the lateral region, while in the bottom region, they were on the cylinder's surface. Between days 7 and 14, few PHOSPHO1-positive osteoblasts directly contacted the block in the lateral region, while many were observed on newly formed bone in the bottom region. By day 28, lines of PHOSPHO1-positive osteoblasts were seen in the cylinder's interior. Thus, bone formation was induced earlier in the bottom region, where HAp/Col fibers were parallel, while bone resorption was predominant in the lateral region, where the fiber ends were exposed. These findings suggest that bone resorption and formation were uncoupled in the early stages after HAp/Col block implantation. By day 28, bone remodeling had shifted to a coupling between osteoclasts and osteoblasts, with neither resorption nor formation dominating in either region.

Conclusions: The orientation of HAp/Col fibers in the HAp/Col block significantly affects whether bone resorption or formation is preferentially induced during the early stages of bone regeneration.

354 words

Keywords: ***bone prosthetic material, hydroxyapatite, collagen, osteoblasts, osteoclasts***

Introduction

Calcium phosphate-based materials have long been used as bone substitute materials for grafts. Bone substitutes containing collagen fibers in addition to calcium phosphate have been developed to more closely mimic the properties of the bone matrix *in vivo*. However, in most cases, successful bone regeneration following bone grafting primarily depends on the characteristics of the calcium phosphate components (size, property, geometrical structure, etc.), while collagen fibers have been considered auxiliary, contributing mainly to cell adhesion and migration. However, the bone matrix consists of a 1:1 volume ratio, corresponding to an approximately 73:27 mass ratio, of hydroxyapatite (HAp) to collagen *in vivo*, so it is feasible that collagen fibers play a significant role in bone formation and regeneration. The collagen fiber arrangement differs significantly between mature cortical bone and immature bone, such as primary trabeculae [1]. Therefore, it is crucial to consider the geometric arrangement of collagen fibers when evaluating bone regeneration using calcium phosphate-based bone grafts containing collagen fibers. However, the orientation of collagen fibers within bone grafts has historically received little attention.

The degree of mineralization of collagen fibers in the bone matrix may depend on the individual age and the position of bone in the body. For instance, immature bone, such as the primary trabeculae beneath the growth plate cartilage during development and growth, exhibits a histologically immature structure with randomly dispersed collagen fibrils [1], and therefore, lacks a lamellar bone structure. In contrast, cortical bone, which forms the thick outer wall of long bones, exhibits a lamellar structure with bundled of collagen fibers regularly arranged in the lamellar layers [2]. In addition, HAp nanocrystals in bone aligned along collagen molecules, *i.e.*, *c*-axes of HAp nanocrystals align to long-axes of collagen molecules and mineral surface of bone is *m*-surface (generally mentioned as *a*-surface but crystallographically correct name is *m*-surface; therefore, in this paper, the authors use correct name.). [3] Nakano et al. demonstrated through X-ray diffraction analysis that the c-axes of hydroxyapatite (HAp) crystals align parallel to the long axis of collagen fibers in mature bone [4]. Moreover, Hasegawa et al. used ultrastructural analysis via transmission electron microscopy to reveal that HAp crystals, which are needle-like in shape and similar in length to the periodic banding of collagen fibers, are consistently and precisely aligned along the direction of the collagen fibers [5]. Thus, HAp crystal face along with collagen fibers may also have some effect on bone formation and bone regeneration.

In cortical bone, not all collagen fibers run in the same direction. Instead, collagen bundles form layers where fibers of approximately equal thickness run in parallel within each layer, creating a plywood-like structure composed of stacked lamellae [2]. Each successive layer of collagen fibers is

oriented at a slight angle relative to the one beneath, forming the lamellar structure of cortical bone. In light of these findings, the HAp and Collagen (HAp/Col) bone substitute developed by Kikuchi et al. appears to closely mimic the distribution and arrangement of collagen fibers and HAp in authentic cortical bone, maintaining a layered structure akin to that observed in native cortical bone, though the collagen fibers exhibit a multidirectional alignment in two dimensions [6]. There are many calcium phosphate-based bone substitutes with collagen fibrils, and the fine structure differs among them. For example, when Bio-Oss Collagen (Bio-Oss®; Geistlich Pharma AG, Wolhusen, Switzerland)—which consists of 10% collagen derived from porcine skin and 90% Bio-Oss granules, making it structurally different from the HAp/Col produced by Kikuchi—is applied to humans, the collagen component is resorbed within 2–3 weeks [7]. Collagraft® (Zimmer Biomet [8]), composed of 60% HAp, 40% tricalcium phosphate, and fibrillar collagen, as well as BONEJECT® (GC Corporation), which combines bovine-derived HAp particles with an atelocollagen solution in a 3:2 weight ratio, are also structurally different from Kikuchi's HAp/Col. The HAp/Col composite can be fabricated in dense, porous, and sheet-like forms [6, 9, 10]. Therefore, it is possible to laminate layers of HAp/Col to form a HAp/Col cylinder with a laminate structure consisting of horizontally aligned collagen fibers in stacked sheets.

In this study, by embedding layered HAp/Col cylinders with aligned collagen fiber bundles into the cortical bone of rat tibiae, we examine whether collagen fiber orientation influences the distribution of osteoclasts and osteoblasts in regions where the fibers run perpendicular or parallel to the bone structure and assess new bone formation during bone regeneration.

Materials and Methods

Preparation of HAp/Col block for bone substitute

Water used in HAp/Col synthesis is water for injection (Otuska Pharmaceutical, Japan) to avoid contamination of endotoxin from water. The HAp/Col bone-like nanocomposite fibers were synthesized by the simultaneous titration method previously reported in the literature [6]. Briefly, 199.1 mmol of $Ca(OH)_2$ (prepared by hydration of CaO obtained from heat decomposition of alkaline analysis grade $CaCO_3$ purchased from Fuji Film Wako Pure Chemical, Ind., Japan) dispersed in 2 dm^3 of H_2O and 59.7 mmol H_3PO_4 (Reagent grade, Fuji Film Wako Pure Chemical, Ind., Japan) aqueous solution containing 5 g of atelocollagen (derived from porcine dermis, Nitta Gelatin, Inc., Japan) were simultaneously and gradually added through respective tube pumps into a central reaction vessel with 1 dm^3 of H_2O previously added. The starting materials were prepared for the composition of the final HAp/Col composite to be 80/20 in mass ratio. The reaction temperature was controlled by a water bath, and the pH of the reaction solution by an automatic titration unit; the water bath temperature was set at 40°C, and reaction pH at 9.0±0.1. The precipitates were filtrated with suction, washed 3 times with H_2O.

The HAp/Col disk with maintaining lamellar fiber structure was prepared by a uni-axial compression of the fibrous precipitate. The HAp/Col fibrous precipitate of 32.6 g was packed in a specially designed mold for water-squeeze forming, and uni-axially compressed at 20 MPa for 24 h to remove excess water and to form into disk of 35 mm in diameter and 3.64 mm in thickness. Three-millimeter-diameter HAp/Col cylinders were prepared by punched out from the disk with a 3-mm punch for leather, were then dried in vacuum and sterilized with ethylene oxide gas.

Animals and the preparation of bone defects and grafts

The HAp/Col cylinders were implanted into the anterior region of the tibia of rats, as shown in **Figure 1**. Thirty 10-week-old male Wistar rats (Japan SLC Co. Inc., Shizuoka, Japan) were handled according to Hokkaido University's guidelines for animal care and research use (approved study protocol #23-0095). The rats were anesthetized with a mixture of 0.3 mg/kg of medetomidine, 4.0 mg/kg of midazolam, and 5.0 mg/kg of butorphanol. After partially shaving the right tibial region, a round cavity defect 1.5‑2.0 mm in diameter was created in the arterial center of the right tibia using a round bur (MS steel bar 016 #5, D+Z Co. Inc., Germany). The site was irrigated with sterilized physiological saline during drilling to prevent overheating. With the defect completed, an HAp/Col cylinder was placed into the defect such that the top and bottom planes of the cylinder and the collagen fiber layers were parallel to the periosteal surface of the tibia **(Fig. 1)**. The defects were covered with the tibial

skin and an instant adhesive (Aron Alpha®, TOAGOSEI, Co. Ltd., Tokyo, Japan).

Specimen preparation

At 3, 5, 7, 14, and 28 days after the HAp/Col grafting ($N = 6$ for each), the rats were anesthetized with the excessive mixture of medetomidine, midazolam butorphanol for bodyweight determination. Then, the rats were perfused with 4% paraformaldehyde diluted in 0.1 M phosphate buffer (pH 7.4) through the left cardiac ventricle, and the tibiae were extracted and immediately immersed in the same solution for 24 h at 4°C. Micro-CT images of all specimens were taken as described below. Then, the treated tibiae were decalcified with 10% EDTA-2Na solution for 2 months. The decalcified specimens were dehydrated in a series of ethanol solutions with increasing concentrations, soaked in xylene, and finally embedded in paraffin. Afterward, 5 μm-thick sagittal paraffin sections were cut to examine two regions of the HAp/Col cylinder: the lateral region facing the cortical bone (perpendicular to the HAp/Col layers), and the bottom region (near the marrow, parallel to the collagen layers) as previously described [11, 12].

Micro-CT analysis

Micro-CT images were obtained from the grafted areas surrounding the cortical bone facing the bone cavity and 1 mm proximally and distally from the edges of the cavity using a micro-CT unit (tube voltage 90 kV, CosmoScan FX, Rigaku Corporation, Tokyo, Japan) following the methods in Morimoto et al. [12]. The CT analyzer software CosmoScan Viewer (Rigaku Corporation, Tokyo, Japan) was employed for image reconstruction per the guidelines described by Bouxsein et al. [13].

Histochemistry for PHOSPHO1 and tartrate-resistant acid phosphatase

After inhibition of endogenous peroxidase activity with methanol containing 0.3% hydrogen peroxidase for 30 min, dewaxed paraffin sections were pretreated with 1% bovine serum albumin (BSA; Serologicals Proteins Inc. Kankakee, IL) in PBS (1% BSA-PBS) for 30 min. The sections were then incubated with rabbit polyclonal anti-PHOSPHO1 antibody (phosphoethanolamine/phosphocholine phosphatase 1; No. Q8TCT1, Cusabio Technology Llc., Houston, TX) diluted at 1:100 in 1% BSA-PBS at room temperature (RT) for 2 h and then incubated with horseradish peroxidase (HRP)-conjugated goat anti-rabbit IgG antibody (P0399, DakoCytomation, Glostrup, Denmark) at a dilution of 1:100 for 1 h at RT. Detection of tartrate-resistant acid phosphatase (TRAP) was conducted as previously described [14]. In brief, the sections were incubated in a mixture of 8 mg of naphthol AS-BI phosphate (Sigma-Aldrich, St. Louis, MO), 70 mg of red-violet LB salt (Sigma-Aldrich), and 50 mM L(+) tartaric acid (0.76g, Nacalai Tesque,

Kyoto, Japan) diluted in 0.1 M sodium acetate buffer (pH 5.0) for 20 min at 37°C, after which the red markings of TRAP activity were visible under light microscopy.

Regions of interest and counting the number of TRAP-positive osteoclasts and PHOSPHO1-reactive osteoblasts

As shown in **Figure 1**, two 300 × 900 μm rectangular regions of interest (ROIs), one located in the center of the distal side of the HAp/Col cylinder and the other in the center of the bottom (marrow) side, were placed in images of the sagittal sections of tibiae to represent regions where the collagen layers of the cylinder run perpendicular and parallel to the bone structure, respectively.

The numbers of TRAP-positive osteoclasts attached to the HAp/Col surface and newly formed bone were counted, as were the total numbers of TRAP-positive osteoclasts in the two ROIs. We regarded TRAP-positive cells with more than two nuclei as osteoclasts. To assess mature osteoblast formation, we counted the PHOSPHO1-reactive osteoblasts localized on the HAp/Col surface and newly formed bone in the ROIs as described recently in Haraguchi-Kitakamae et al. [15].

Statistical analysis

All values are expressed as means ± standard errors. Student's *t*-tests were used for two-group comparisons, and one-way ANOVAs followed by Dunnett's tests were used for multiple comparisons. In all tests, *P*-values < 0.05 were considered to infer statistical significance. All data were analyzed using BellCurve for Excel version 4.07 (Social Survey Research Information Co., Ltd., Tokyo, Japan).

Results

Micro-CT imaging

The micro-CT images of the HAp/Col cylinder from day 3 to day 28 after grafting revealed that the upper surfaces of the cylinders were nearly parallel to the surface of the surrounding cortical bone **(Fig. 2)**. By day 5, a semi-transparent tissue that was not visible on day 3 had formed around the HAp/Col cylinders. This semi-transparent tissue seemed continuous with the cortical bone on both the lateral and bottom (marrow) surfaces of the cylinder **(Fig. 2B)**. By day 7, the semi-transparent tissue had thickened enough to be recognized as new bone tissue **(Fig. 2C)**. On day 14, radiopaque trabecular bone had become more apparent around the HAp/Col cylinder, with the surface of the cylinder appearing rougher **(Fig. 2D)**. On day 28, the cortical bone adjacent to the cylinder and the HAp/Col cylinder seemed osseo-integrated, whereas in the bottom regions, the HAp/Col cylinder had been resorbed **(Fig. 2E)**.

Chronological observations on the history after HAp/Col cylinder grafting

On day 3, the surface of the grafted HAp/Col cylinders was smooth, with bone marrow tissue surrounding the cylinders **(Fig. 3)**. In the lateral region, a small amount of cellular invasion into the cylinder was observed, with cells aligned in one or two rows **(Fig. 3A, B)**. By day 5, fine trabecular bone had formed around the HAp/Col cylinder **(Fig. 3D)**. A thick layer of cells surrounded the lateral surface, and though trabeculae were not continuous with the cylinder surface, immature trabeculae had been formed at a distance from the surface **(Fig. 3E)**. On the bottom surface of the cylinder, a network of trabeculae was seen extending continuously from the surface **(Fig. 3F)**. On day 7, the HAp/Col cylinder was surrounded by newly formed bone with a typical structure of trabeculae **(Fig. 3G)**. Under higher magnification, trabeculae were verified to be formed at some distance from the HAp/Col cylinder in its lateral region, with fibrous stromal tissue intervening between the HAp/Col cylinder and the trabeculae **(Fig. 3H)**. In contrast, at the bottom surface of the HAp/Col cylinder, a thin layer of bone matrix was covered, from which numerous trabeculae extended outward **(Fig. 3I)**. On day 14, the HAp/Col cylinder exhibited a rough, uneven surface **(Fig. 3J)**. Continuity between the newly formed bone and the HAp/Col cylinder was still not observed in the lateral region. Notably, numerous multinucleated giant cells were localized on the lateral surface of the HAp/Col cylinder **(Fig. 3K)**. Additionally, a row of cells had invaded the inside of the cylinder in an almost parallel arrangement. Though continuity between the cortical bone and the HAp/Col cylinder had still not been established, a thick layer of the stromal tissues with bone marrow had developed between the cylinder and the surrounding trabecular bone. In contrast, the bottom region of the cylinder had become fragmented

into islands, with newly formed bone filling the spaces between them. Multinucleated giant cells were also observed at the boundary between the HAp/Col and new bone tissues **(Fig. 3L)**. By day 28, the shape of the HAp/Col cylinder had collapsed, and newly formed bone had penetrated its interior **(Fig. 3M)**. In the lateral region, newly formed bone extending from the cortical bone had invaded into the cylinder, indicating integration between the HAp/Col and new bone tissues **(Fig. 3N)**. In the bottom region, numerous multinucleated giant cells had accumulated, indicative of active bone resorption **(Fig. 3O)**.

Chronological distribution of TRAP-positive osteoclasts

On day 3, quite a few TRAP-positive osteoclasts were observed around the HAp/Col cylinder **(Fig. 4A)**. At this point, few TRAP-positive cells were seen on the lateral region relative to the bottom region **(Fig. 4B, C)**. On day 5, TRAP-positive osteoclasts tended to be localized across the lateral surface of the cylinder **(Fig. 4D, E)**, with fewer observed on the bottom surface **(Fig. 4F)**. By day 7, many TRAP-positive osteoclasts were localized on the lateral surface of the HAp/Col cylinder, and some had invaded the cylinder's interior **(Fig. 4G, H)**. At the bottom region, in contrast, only a few TRAP-positive osteoclasts were observed **(Fig. 4I)**. On day 14, a large number of TRAP-positive osteoclasts were again observed on the lateral surface of the cylinder, with many invading the superficial areas **(Fig. 4J, K)**. In addition, the newly formed bone tissue adjacent to the lateral surface of the cylinder also contained many TRAP-positive osteoclasts **(Fig. 4K)**. In the bottom region, TRAP-positive osteoclasts were observed on the newly formed trabeculae **(Fig. 4L)**. By day 28, TRAP-positive osteoclasts had completely invaded the HAp/Col cylinder, with strong indications of resorption by osteoclasts on both the lateral and bottom surfaces **(Fig. 4M–O)**.

Statistical analysis of the distribution of TRAP-positive osteoclasts

We analyzed the numbers of osteoclasts attached to the HAp/Col and newly formed bone, as well as the total number of osteoclasts in the ROIs **(Fig. 5)**. On day 3, in both osteoclast measures, only a few TRAP-positive osteoclasts were observed around the HAp/Col cylinder, with no differences between regions. From days 5 to 14, the number of osteoclasts attached to the HAp/Col cylinder/newly formed bone and the total number of osteoclasts increased significantly over time, particularly in the lateral region, where the collagen fiber layers intersect. However, in the bottom region, while the number of osteoclasts increased, this increase was less pronounced compared to the lateral region. By day 28, however, the number of osteoclasts attached to the cylinder and new bone had decreased in the lateral region to that of the bottom region. In contrast, the total number of osteoclasts was still higher in the lateral region than in the bottom region. Thus, it is likely that osteoclasts predominantly accumulate in

the lateral region, where the collagen fiber layers intersect, rather than in the bottom region, where the collagen fibers run parallel.

Chronological distribution of PHOSPHO1-positive osteoblasts

Three days after the graft surgery, PHOSPHO1-positive osteoblasts were not observable on the surface of the HAp/Col cylinder **(Fig. 6A–C)**. On days 5−7, PHOSPHO1-positive osteoblasts were seen in the trabecular bones around the HAp/Col cylinder **(Fig. 6D, G)**. In the lateral regions of the HAp/Col cylinder, PHOSPHO1-positive osteoblasts were seen in the trabecular bone away from the cylinder surface, but no PHOSPHO1-positive osteoblasts were detected on the surface **(Fig. 6E, H)**. In contrast, PHOSPHO1-positive osteoblasts were detected in the new bone tissue extending from the bottom surface of the cylinder **(Fig. 6F, I)**. Fourteen days after grafting, PHOSPHO1-positive osteoblasts were still present in the trabecular bone at a distance from but not on the lateral surface of the HAp/Col cylinder **(Fig. 6J, K)**. In contrast, lines of PHOSPHO1-positive osteoblasts were noted on the newly formed trabecular bone in the bottom region **(Fig. 6L)**. By 28 days, rows of PHOSPHO1-positive osteoblasts had extended throughout the HAp/Col cylinder **(Fig. 6M, N)**. Conversely, PHOSPHO1-positive osteoblasts showed a decreasing trend in the trabecular bone at the bottom region of the cylinder **(Fig. 6O)**.

Statistical analysis of the distribution of PHOSPHO1-positive osteoblasts

We counted the numbers of PHOSPHO1-positive osteoblasts attached to the HAp/Col cylinder and the newly formed bone in the ROIs of the lateral and bottom regions **(Fig. 7)**. During days 5–14 days, PHOSPHO1-positive osteoblasts predominantly increased in the bottom region when compared with the lateral region, showing significantly greater numbers throughout this period. However, by the 28th day, there was no significant difference in the numbers of PHOSPHO1-positive osteoblasts between the lateral and bottom regions.

Discussion

We aimed to clarify whether the orientation of collagen fibers in a bone substitute material composed of HAp and collagen fibers affects bone resorption and bone formation. To achieve this, we implanted an HAp/Col graft composed of layered collagen plates into the diaphysis of rat tibiae and conducted histological analyses. Our results showed that the lateral region (where the collagen fiber ends are exposed) and the bottom region (where the collagen fibers run parallel) induced different patterns of osteoclast and osteoblast localization during the early period (5–14 days) after implantation. Specifically, in the lateral region, a large number of osteoclasts accumulated on the surface of the HAp/Col cylinder, with little localization of osteoblasts, while in the bottom region, osteoblastic bone formation was predominant over osteoclast accumulation **(Fig. 8)**. These findings suggest that the orientation of collagen fibers influences the early localization of osteoclasts and osteoblasts, which affects bone modeling, *i.e.*, an uncoupling of osteoclastic bone resorption and/or osteoblastic bone formation, and implies significant implications for bone regeneration.

Hydroxyapatite and beta-tricalcium phosphates are well-known osteoconductive materials that serve as scaffolds for the migration and attachment of bone cells [16-21]. Research suggests that the replacement of bone substitute material with newly formed bone is carried out in accordance with bone remodeling: First, osteoclasts resorb the osteoconductive calcium phosphate-based bone substitute material. This is followed by the migration of osteoblasts, which then add bone matrix [21, 22]. These findings implicate a phenomenon mimicking bone remodeling but not bone modeling, even during bone regeneration.

To facilitate cell infiltration into calcium phosphate-based bone substitutes, various improvements have been made. One such improvement has been an optimization of the granule and pore sizes of the substitute. Another was the incorporation of collagen fibers, such as atelocollagen, into calcium phosphate-based bone substitutes [23-27]. However, the orientation of collagen fibers has received relatively little attention. Therefore, we examined how the orientation of collagen fibers in a bone substitute affected bone resorption and formation. To do this, it is necessary to exclude other factors that would induce bone resorption and bone formation, for instance, mechanical stress and the osteocytic lacunar canalicular system [28-30]. Therefore, we embedded the HAp/Col graft avoiding tight contact between the embedded cylinders and pre-existing bone tissue around the bone cavity defect in the rat tibiae, as verified by the micro-CT images. In addition, there was no living osteocytic network in the HAp/Col cylinder. Therefore, we believe that our study excluded the possible effects of internal mechanical stress to the HAp/Col cylinders. We hypothesize that, in the absence of mechanical

stress, the orientation of collagen fibers may affect the localization of osteoclast and osteoblast accumulation.

One may wonder “Why did osteoclasts accumulate in the graft’s lateral region, where the fiber ends are exposed at the surface, while bone formation by osteoblasts was induced in the bottom region, where the collagen fibers run parallel to the surface?” According to the studies by Hasegawa et al. [31], osteoblast projections show two types: one that extends perpendicularly to the bone surface to connect with osteocytes and another that encompasses collagen bundles. Therefore, there is a relationship between the orientation of osteoblast projections and that of collagen fiber bundles, and the present study’s findings suggest that HAp/Col fibers parallel to the secretion surface of osteoblasts may be more advantageous, *e.g.,* for cell adhesion via integrins [32]. On the other hand, the bone resorption compartment of osteoclasts, which is also responsible for collagen reabsorption, has a characteristic ruffled border, and it seems that collagen fibers oriented perpendicularly to this resorption surface may be more easily absorbed. In addition, several researchers mentioned that HAp crystals have different properties depending on their surface orientation. Specifically, the m-surface and c-surface of HAp exhibit differences in crystal solubility, protein adsorption, and cell growth [33,34]. Aizawa et al demonstrated that osteoblasts promoted mineralization when cultured on HAp ceramics with m-surface orientation *in vitro* [35]. In our study, the bottom surface of HAp/Col cylinders aligned with the m-surface of HAp crystals induced osteoblastic bone formation. These findings indicated that both the orientation of collagen fibers and HAp crystals may contribute to osteoblast induction.

The distinct osteoclast and osteoblast accumulation patterns associated with the different HAp/Col fiber orientations were most pronounced in the early stages of graft recovery in this study. As bone resorption and bone formation progress, the distribution of osteoclasts and osteoblasts within the HAp/Col cylinder became scattered over time. This is likely due simply to the nature of the bone remodeling process, which has previously been described [36, 37]. Therefore, in the context of bone reconstruction, if the orientation of collagen fibers in the HAp/Col graft can be standardized to induce osteoclast or osteoblast accumulation in desired areas, it may be possible to guide bone regeneration in a controlled manner during the early stages.

One limitation of this study is that, while the HAp/Col fibers were aligned in one plane, they still pointed in various directions within that plane, meaning that the structure did not fully mimic the geometric structure of lamellar bone tissue, such as that of cortical bone. Based on these results, further improvements in the design of HAp/Col grafts with refined collagen fiber orientations are anticipated. Regarding the enumeration of TRAP-positive osteoclasts and osteoblasts, especially in the late stages, it was hard to distinguish osteoclast/osteoblasts located on the HAp/Col surface from those on the newly formed bone. Therefore, in this study, we counted the osteoclasts/osteoblasts located on the

cylinder and the new bone together. Additionally, further analysis is required to elucidate the mechanisms by which collagen fiber alignment and HAp crystal face induces the distinct localizations of osteoclasts and osteoblasts.

Conclusions

The results of this study suggest that when an HAp/Col graft with HAp/Col fibers in a planar orientation is implanted into the tibial cavity of rats, osteoclasts accumulate in the region where the collagen fiber ends are exposed, while osteoblasts tend to adhere and induce bone formation in the regions where the collagen fibers run parallel to the bone tissue's surface. In bone reconstruction, controlling the orientation of collagen fibers in HAp/Col bone substitute materials may allow for targeted bone resorption or the promotion of bone formation in specific regions, potentially enabling surgeons to guide bone regeneration in a predictable manner.

Ethical standards

All animal experiments were performed in accordance with the Japanese Act on Welfare and Management of Animals. The protocol was approved by the Institutional Animal Care and Use Committee of Hokkaido University (approved research proposal #23-0095).

Competing interests

The authors declare no competing interests.

Contributors

Hasegawa T and Kikuchi M designed this study and prepared the final draft of the article. Sakakibara M is the first author in charge of writing the original draft and analyzing and interpreting the data. Haraguchi-Kitakamae M, Shi Y, Li W, Liu X, and Hongo H contributed to the histochemical analysis. Cui J and Yamamoto T worked on the statistical analyses and critically read the manuscript. Sato Y and Amizuka N participated in the discussion, editing, and formatting of the manuscript.

Reference

[1] Shapiro F, Wu JY. Woven bone overview: structural classification based on its integral role in developmental, repair and pathological bone formation throughout vertebrate groups. ***Eur Cell Mater.*** 38:137-167, 2019.

[2] Yamamoto T, Hasegawa T, Hongo H, Amizuka N. Alternating lamellar structure in human cellular cementum and rat compact bone: Its structure and formation. ***J Oral Biosci.*** 61(2):105-114, 2019.

[3] Sasaki, N. and Sudoh, Y.: X-ray pole figure analysis of apatite crystals and collagen molecules in bone. ***Calcif Tissue Int***. 60, 361-367, 1997.

[4] Nakano T, Kaibara K, Tabata Y, Nagata N, Enomoto S, Marukawa E, et al. Unique alignment and texture of biological apatite crystallites in typical calcified tissues analyzed bymicrobeam X-ray diffractometer system. ***Bone.*** 31(4):479-87, 2002.

[5] Hasegawa T, Li M, Hara K, Sasaki M, Tabata C, Freitas PHL, et al. Morphological assessment of bone mineralization in tibial metaphyses of ascorbic acid-deficient ODS rats. ***Biomed Res.*** 32(4):259-269, 2011.

[6] Kikuchi M, Itoh S, Ichinose S, Shinomiya K, Tanaka J. Self-organization mechanism in a bone-like hydroxyapatite/collagen nanocomposite synthesized in vitro and its biological reaction in vivo. ***Biomaterials.*** 22: 1705-1711, 2001.

[7] Wang J, Cui W, Zhao Y, Lei L, Li H. Clinical and radiographic evaluation of Bio-Oss granules and Bio-Oss Collagen in the treatment of periodontal intrabony defects: a retrospective cohort study. ***J Appl Oral Sci.*** 32: e20230268, 2024.

[8] Cornell CN, Lane JM, Chapman M, Merkow R, Seligson D, Henry S, et al.Multicenter trial of Collagraft as bone graft substitute. ***J Orthop Trauma*** 5(1):1-8, 1991.

[9] Kikuchi M, Ikoma T, Syoji D, Matsumoto HN, Koyama Y, Itoh S, et al. Porous body preparation of hydroxyapatite/collagen nanocomposites for bone tissue regeneration. ***Key Eng Mater.*** 254-256:561-4, 2004.

[10] Kikuchi M. Osteogenic activity of MG63 cells on hydroxyapatite/collagen nanocomposite membrane. ***Key Eng Mater.*** 330-332: 313-6, 2007.

[11] Hasegawa T, Yamamoto T, Sakai S, Miyamoto Y, Hongo H, Qiu Z, et al. Histological Effects of the Combined Administration of Eldecalcitol and a Parathyroid Hormone in the Metaphyseal Trabeculae of Ovariectomized Rats. ***J Histochem Cytochem.*** 67(3):169-184, 2019.

[12] Morimoto Y, Hasegawa T, Hongo H, Yamamoto T, Maruoka H, Haraguchi-Kitakamae M, Nakanishi K, Yamamoto T, Ishizu H, Shimizu T, Yoshihara K, Yoshida Y, Sugaya T, Amizuka N. Phosphorylated pullulan promotes calcification during bone regeneration in the bone defects of rat tibiae. ***Front Bioeng Biotechnol.*** 11:1243951, 2023.

[13] Bouxsein ML, Boyd SK, Christiansen BA, Guldberg RE, Jepsen KJ, Muller R. Guidelines for assessment of bone microstructure in rodents using micro-computed tomography. ***J Bone Min Res.*** 25: 1468–1486, 2010.

[14] Hasegawa T, Tokunaga S, Yamamoto T, Sakai M, Hongo H, Kawata T, et al. Evocalcet rescues secondary hyperparathyroidism-driven cortical porosity in chronic kidney disease male rats. ***Endocrinology.*** 164(4): bqad022, 2023.

[15] Haraguchi-Kitakamae M, Nakajima Y, Yamamoto T, Hongo H, Cui J, Shi Y, et al. Regional difference in the distribution of alkaline phosphatase, PHOSPHO1, and calcein labeling in the femoral metaphyseal trabeculae in parathyroid hormone-administered mice. ***J Oral Biosci.*** 66(3):554-566, 2024.

[16] Block MS, Kent JN. Long-term radiographic evaluation of hydroxylapative-augmented mandibular alveolar ridges. ***J Oral Maxillofac Surg.*** 42: 793–796, 1984.

[17] Bifano CA, Edgin WA, Colleton C, Bifano SL, Constantinoet PD. Preliminary evaluation of hydroxyapatite cement as an augmentation device in the edentulous atrophic canine mandible. ***Oral Surg Oral Med Oral Pathol Oral Radiol Endod.*** 85: 512–516, 1998.

[18] Liljensten E, Adolfsson E, Strid KG, Thomsen P. Resorbable and nonresorbable hydroxyapatite granules as bone graft substitutes in rabbit cortical defects. ***Clin Implant Dent Relat Res.*** 5: 95–102, 2003.

[19] Tapety FI, Amizuka N, Uoshima K, Nomura S, Maeda T. A histological evaluation of the involvement of Bio-OssR in osteoblastic differentiation and matrix synthesis. ***Clin Oral Implants Res.*** 15: 315–324, 2004.

[20] Lee YM, Shin SY, Kim JY, Kye SB, Ku Y, Rhyu IC. Bone reaction to bovine hydroxyapatite for maxillary sinus floor augmentation: histologic results in humans. ***Int J Periodontics Restor Dent.*** 26: 471–481, 2006.

[21] Nakadate M, Amizuka N, Li M, Freitas PHL, Oda K, Nomura S, et al. Histological evaluation on bone regeneration of dental implant placement sites grafted with a self-setting alpha-tricalcium phosphate cement. ***Microsc Res Tech.*** 7: 93–104, 2008.

[22] Kojima T, Amizuka N, Suzuki A, de Freitas PH, Yoshizawa M, Kudo A, et al. Histological examination of bone regeneration achieved by combining grafting with hydroxyapatite and thermoplastic bioresorbable plates. ***J Bone Min Metab.*** 25: 361–373, 2007.

[23] An J, Liao H, Kucko NW, Herber RP, Wolke JG, van den Beucken JJ, et al. Long-term evaluation of the degradation behavior of three apatite-forming calcium phosphate cements. ***J Biomed Mat Res A*** 104: 1072–1081, 2016.

[24] Chang YL, Lo YJ, Feng SW, Huang YC, Tsai HY, Lin CT, et al. Bone healing improvements using hyaluronic acid and hydroxyapatite/beta-tricalcium phosphate in combination: an animal study. ***Biomed Res Int.*** 2016: 8301624, 2016.

[25] Pilliar RM, Kandel RA, Grynpas MD, Theodoropoulos J, Hu Y, Allo B, et al. Calcium polyphosphate particulates for bone void filler applications. ***J Biomed Mater Res B Appl Biomater.*** 105: 874–884, 2017.

[26] Bohner M, Santoni BLG, Döbelin N. β-Tricalcium phosphate for bone substitution: synthesis and properties. ***Acta Biomater.*** 113: 23–41, 2020.

[27] Saito S, Hamai R, Shiwaku Y, Hasegawa T, Sakai S, Tsuchiya K, et al. Involvement of distant octacalcium phosphate scaffolds in enhancing early differentiation of osteocytes during bone regeneration. ***Acta Biomater.*** 129: 309–322, 2021.

[28] Bikle DD, Halloran BP. The response of bone to unloading. ***J Bone Miner Metab.*** 17: 233-44, 1999.

[29] Chen H, Senda T, Kubo KY. The osteocyte plays multiple roles in bone remodeling and mineral homeostasis. ***Med Mol Morphol.*** 48: 61-68, 2015.

[30] Wang L, You X, Lotinun S, Zhang L, Wu N, Zou W. Mechanical sensing protein PIEZO1 regulates

bone homeostasis via osteoblast-osteoclast crosstalk. ***Nat Commun.*** 11: 282, 2020.

[31] Hasegawa T, Yamamoto T, Hongo H, Qiu Z, Abe M, Kanesaki T, et al. Three-dimensional ultrastructure of osteocytes assessed by focused ion beam-scanning electron microscopy (FIB-SEM). ***Histochem Cell Biol.*** 149: 423-432, 2018.

[32] Jokinen J, Dadu E, Nykvist P, Käpylä J, White DJ, Ivaska J, et al. Integrin-mediated cell adhesion to type I collagen fibrils. ***J Biol Chem.*** 279: 31956-63, 2004.

[33] Chen W, Tian B, Lei Y, Ke QF, Zhu ZA, Guo YP. Hydroxyapatite coatings with oriented nanoplate and nanorod arrays: Fabrication, morphology, cytocompatibility and osteogenic differentiation. ***Mater Sci Eng C Mater Biol Appl.*** 67, 395–408, 2016.

[34] Onuma E, Honda T, Yoshimura H, Nishihara T, Ogura A, Kanzawa N, et al. Identification of Proteins Adsorbed on Hydroxyapatite Ceramics with a Preferred Orientation to a-Plane. ***Crystals***. 13, 1318, 2023.

[35] Aizawa M. Development of bioceramics with life functions by harnessing crystallographic anisotropy and their biological evaluations. ***J Ceram Soc Jpn.*** 128, 997–1004, 2020.

[36] Itoh S, Kikuchi M, Takakuda K, Nagaoka K, Koyama Y, Tanaka J, et al. Implantation study of a novel hydroxyapatite/collagen (HAp/col) composite into weight-bearing sites of dogs. ***J Biomed Mater Res.*** 63: 507-15, 2002.

[37] Hiratsuka T, Uezono M, Takakuda K, Kikuchi M, Oshima S, Sato T, et al. Enhanced bone formation onto the bone surface using a hydroxyapatite/collagen bone-like nanocomposite. ***J Biomed Mater Res B Appl Biomater.*** 108: 391-398, 2020.

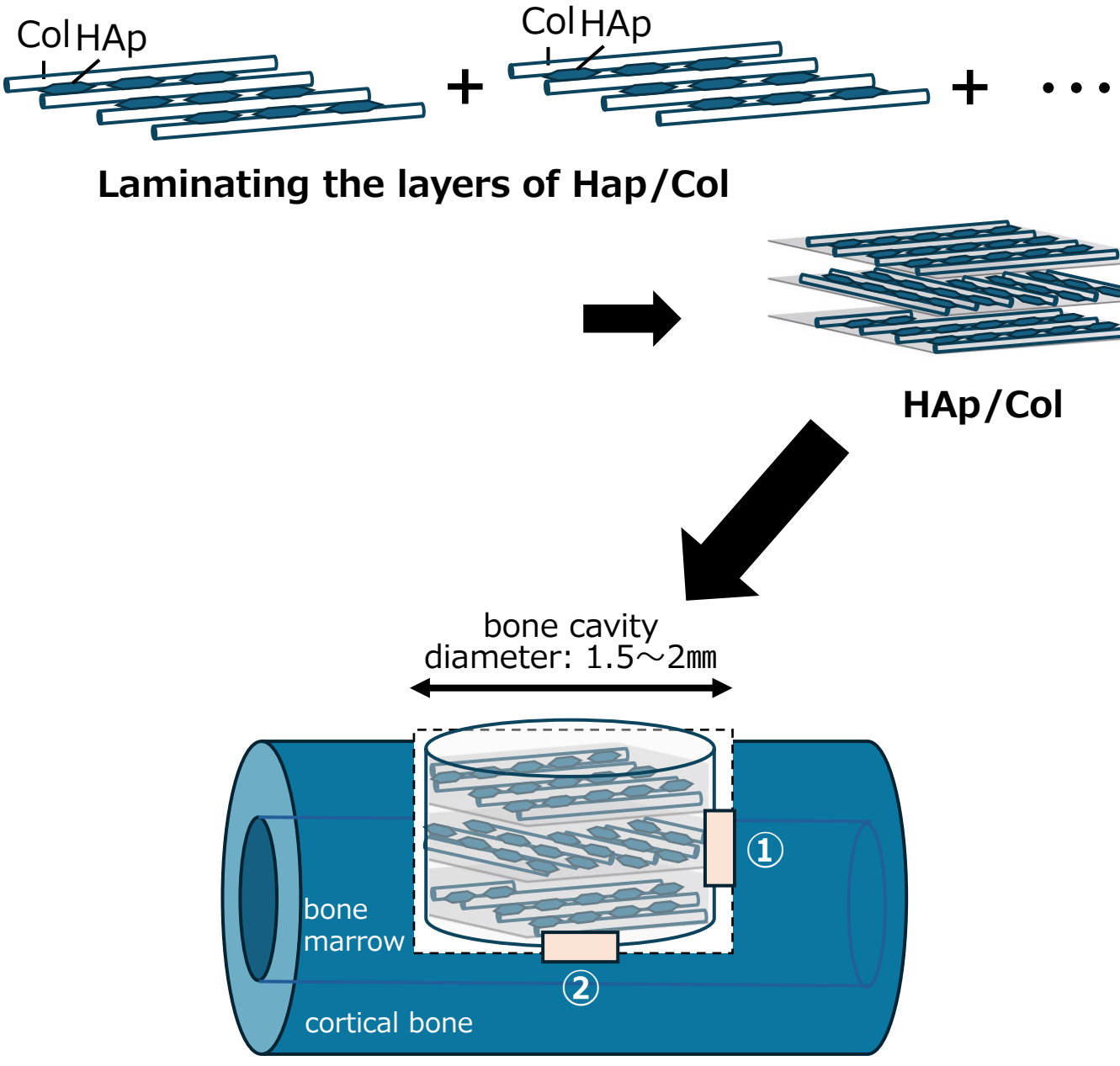

Regions of Interest
① : the region perpendicular to the collagen layers
② : the region parallel to the collagen layers

Figure 1

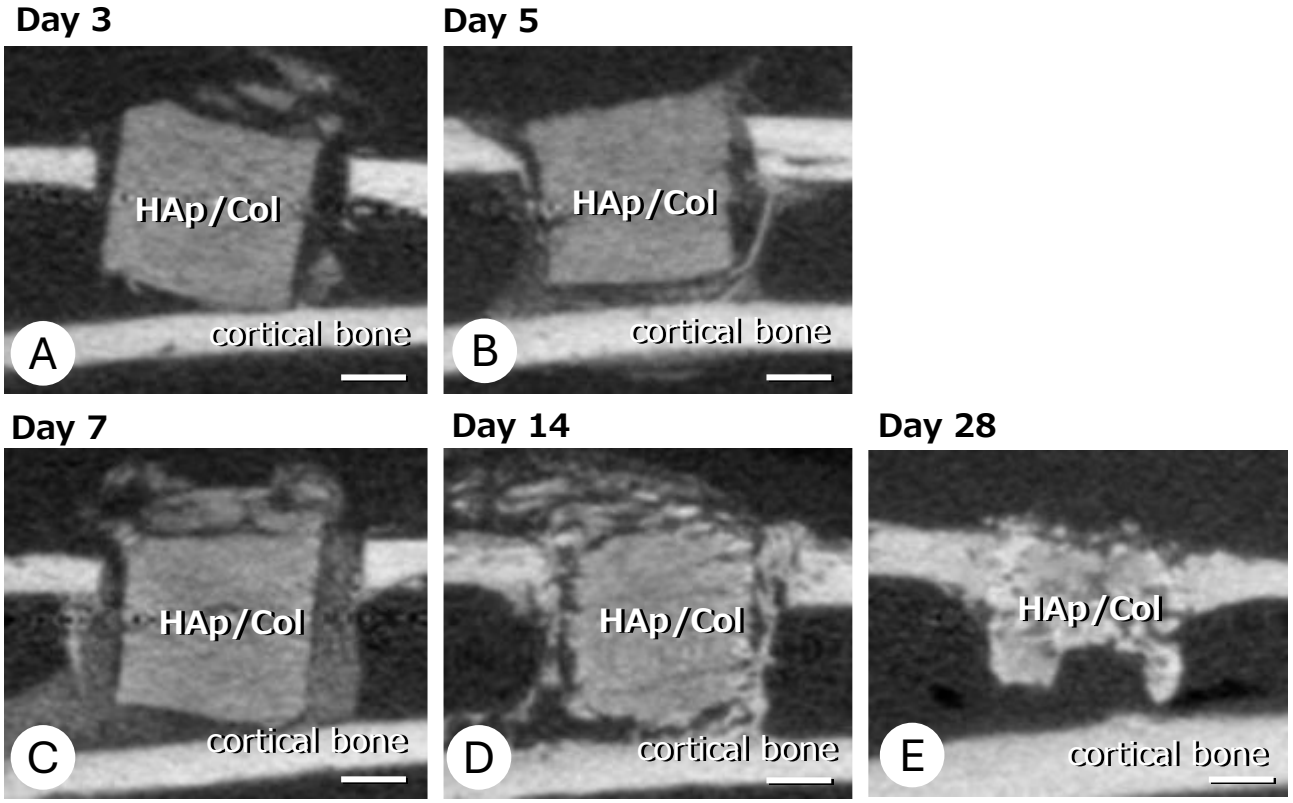
Day 3
HAp/Col
cortical bone
A
Day 5
HAp/Col
cortical bone
B
Day 7
HAp/Col
cortical bone
C
Day 14
HAp/Col
cortical bone
D
Day 28
HAp/Col
cortical bone
E

Figure 2

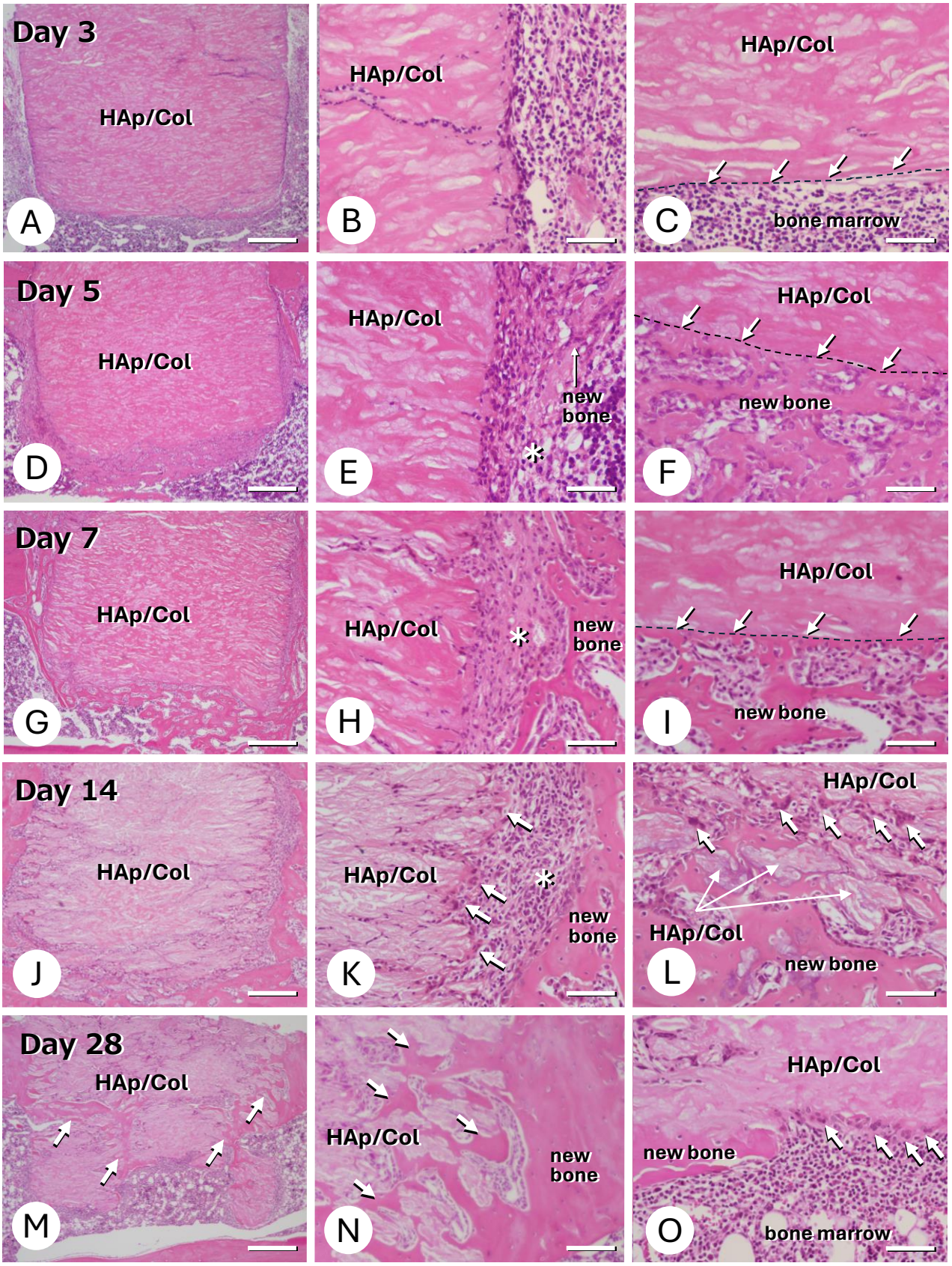
Day 3
HAp/Col
A
HAp/Col
B
HAp/Col
bone marrow
C
Day 5
HAp/Col
D
HAp/Col
new bone
*
E
HAp/Col
new bone
F
Day 7
HAp/Col
G
HAp/Col
*
new bone
H
HAp/Col
new bone
I
Day 14
HAp/Col
J
HAp/Col
*
new bone
K
HAp/Col
HAp/Col
new bone
L
Day 28
HAp/Col
M
HAp/Col
new bone
N
HAp/Col
new bone
bone marrow
O

Figure 3

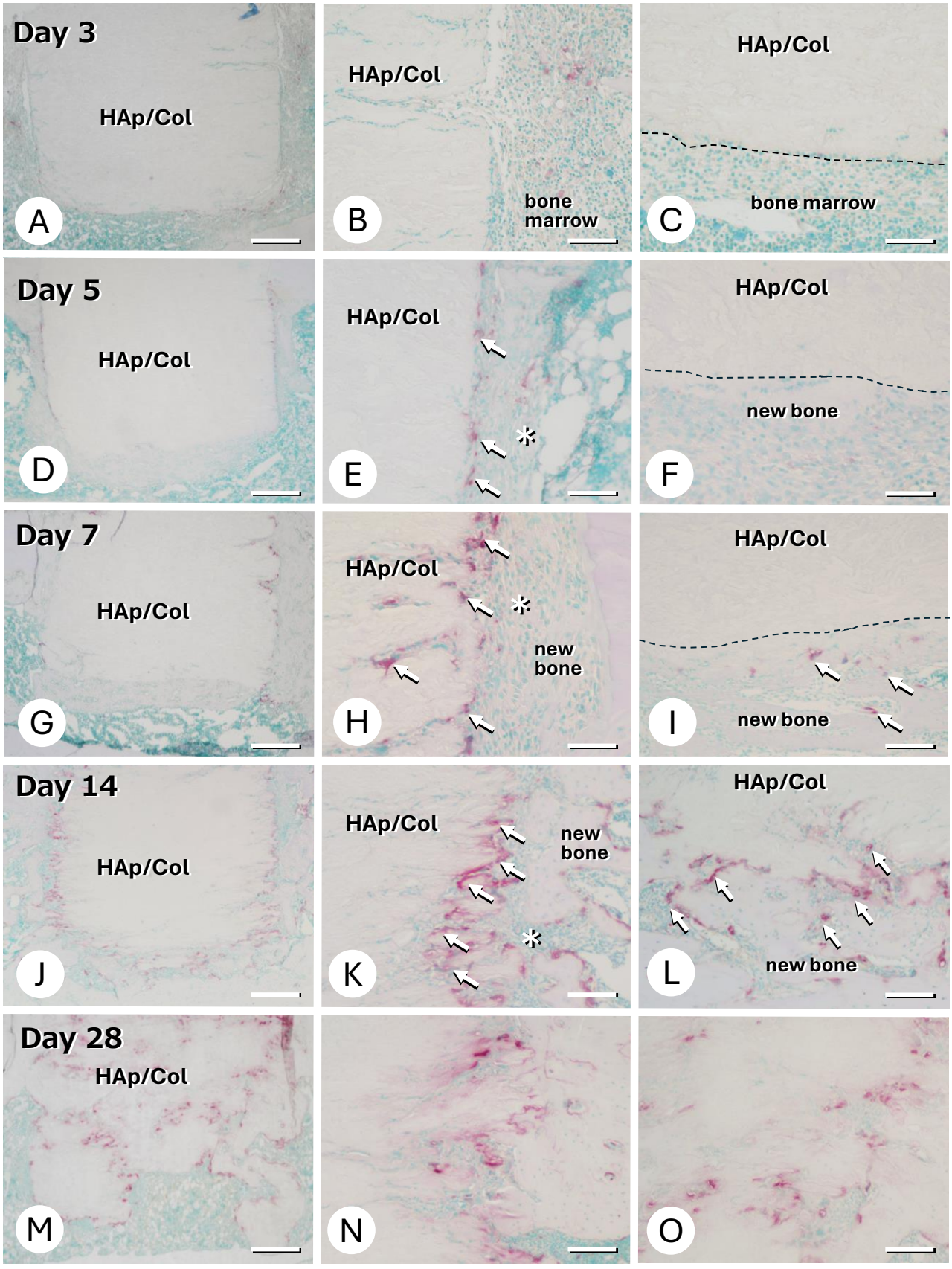
Day 3
HAp/Col
A
HAp/Col
bone
marrow
B
HAp/Col
bone marrow
C
Day 5
HAp/Col
D
HAp/Col
E
HAp/Col
new bone
F
Day 7
HAp/Col
G
HAp/Col
new
bone
H
HAp/Col
new bone
I
Day 14
HAp/Col
J
HAp/Col
new
bone
K
HAp/Col
new bone
L
Day 28
HAp/Col
M
N
O

Figure 4

The numbers of TRAP-positive osteoclasts on the HAp/Col and newly-formed one in ROIs

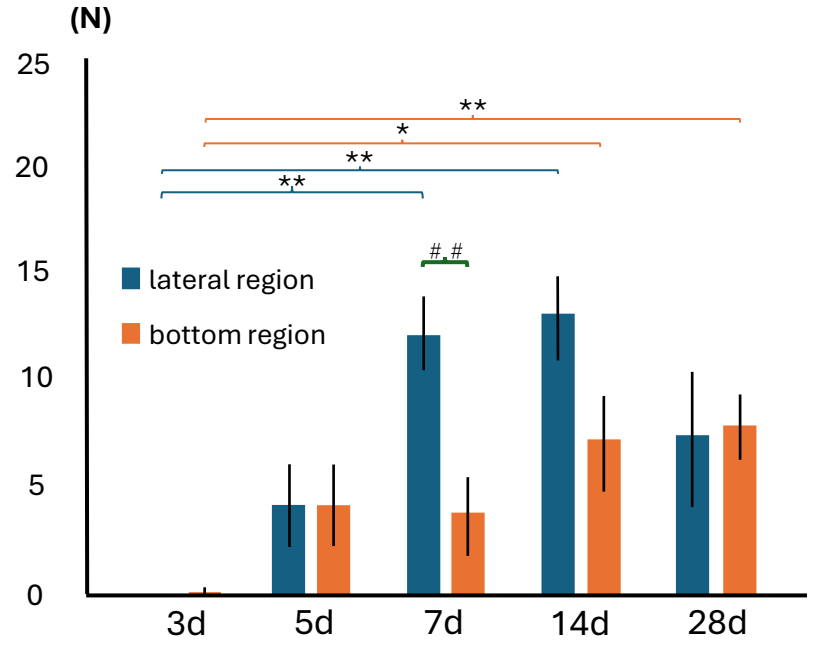

**: p<0.01
*: p<0.05
##: p<0.01

A

The total numbers of TRAP-positive osteoclasts in ROIs

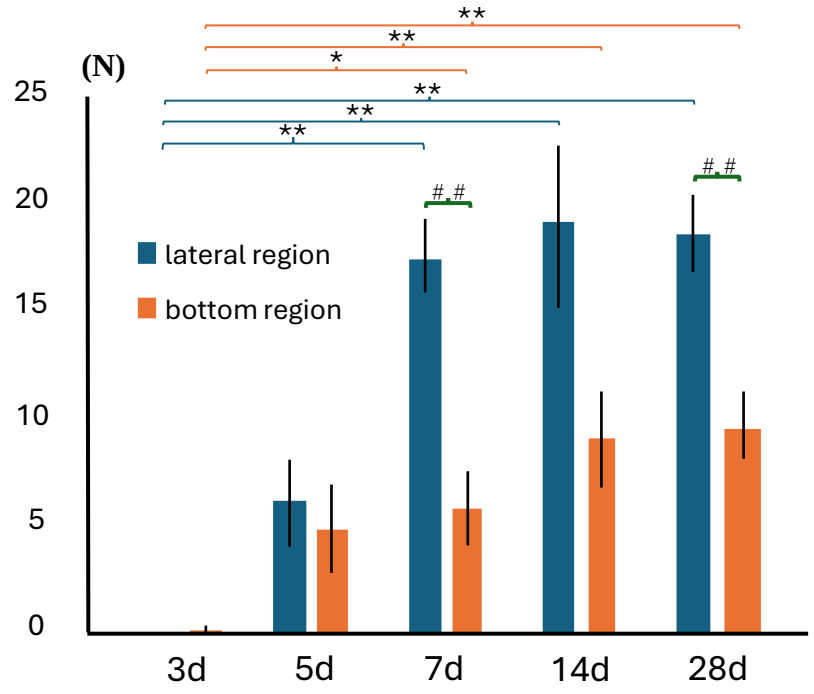

**: p<0.01
*: p<0.05
##: p<0.01

B

Figure 5

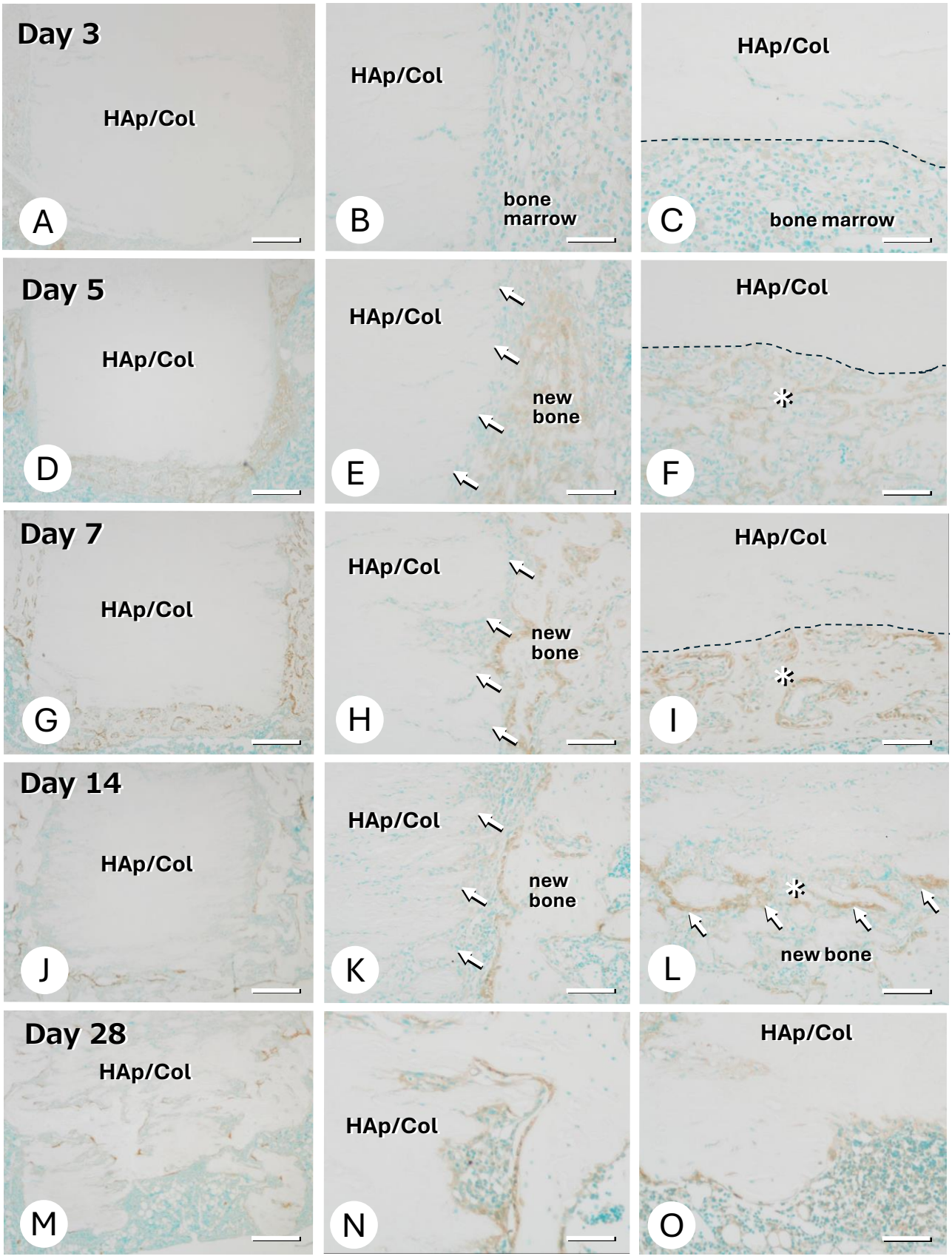
Day 3
HAp/Col
A
HAp/Col
bone
marrow
B
HAp/Col
bone marrow
C
Day 5
HAp/Col
D
HAp/Col
new
bone
E
HAp/Col
F
Day 7
HAp/Col
G
HAp/Col
new
bone
H
HAp/Col
I
Day 14
HAp/Col
J
HAp/Col
new
bone
K
new bone
L
Day 28
HAp/Col
M
HAp/Col
N
HAp/Col
O

Figure 6

The numbers of PHOSPHO1-positive osteoblasts on the HAp/Col and newly-formed one in ROIs

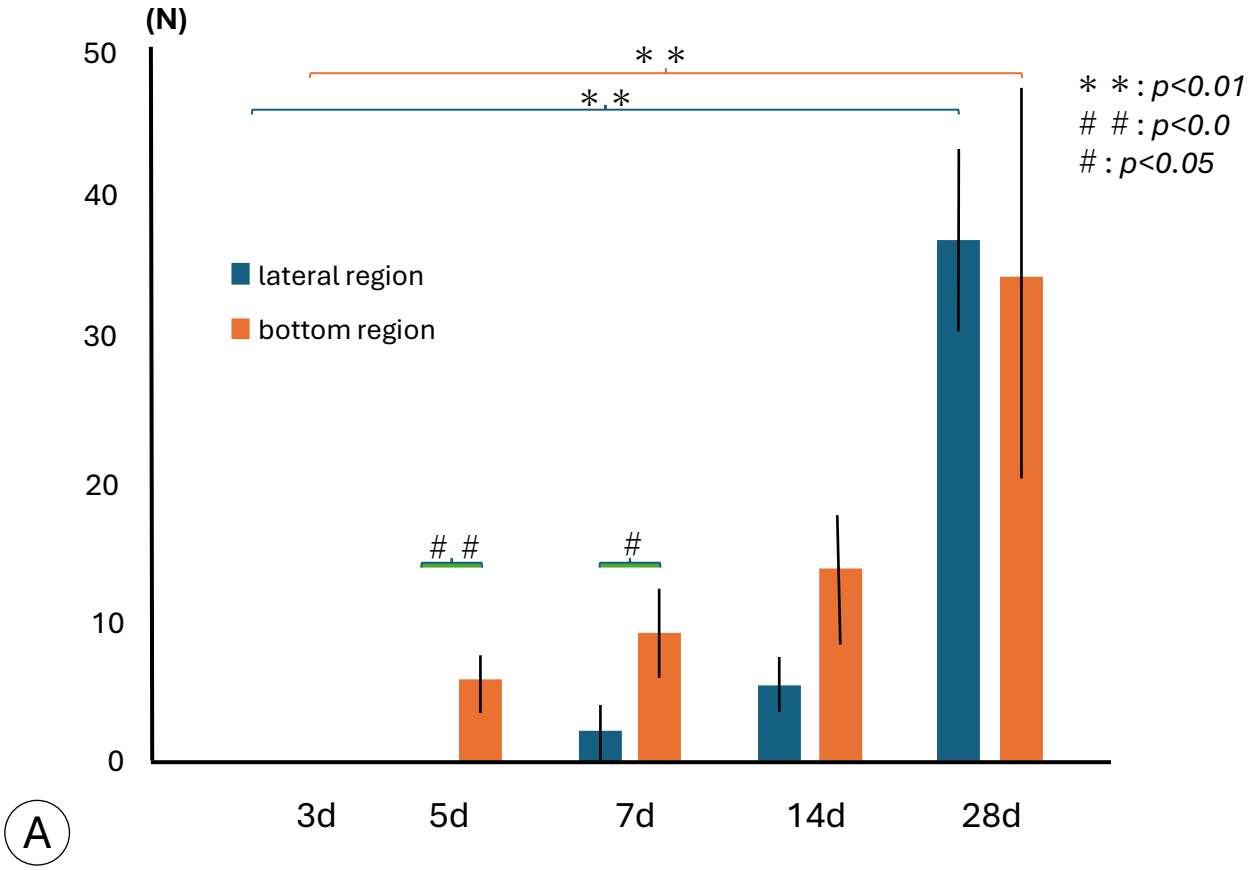

Figure 7

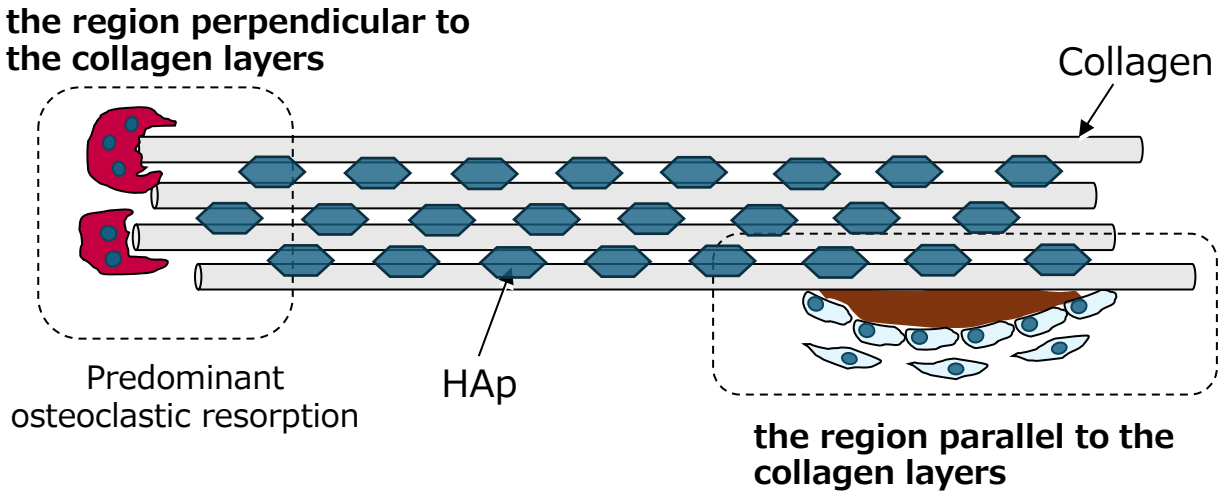
the region perpendicular to
the collagen layers
Collagen
Predominant
osteoclastic resorption
HAp
the region parallel to the
collagen layers

Figure 8

Figure legends

Figure 1

Schematic design of HAp/Col embedding into rat tibiae

A cylinder of HAp/Col with a diameter of 1.5 mm and a height of 1.5 mm was implanted into a 1.5–2.0 mm diameter bone defect in the arterial center of the right tibia of 10-week-old male Wistar rat. Two 300 × 900 μm rectangular regions of interest (ROIs) were set up located in the center of the lateral (perpendicular to the collagen layers) and bottom (parallel to the collagen layers) regions of the HAp/Col cylinder.

Figure 2

Micro-CT images of the HAP/Col cylinder taken 3–28 days after grafting into the bone cavities

The micro-CT images reveal a semi-transparent tissue around the HAp/Col cylinders on days 5 and 7 that was not present 3 days after grafting **(A-C)**. By day 14, trabecular bone is apparent around the cylinder, while the surface appears roughened **(D)**. On day 28, the HAp/Col cylinder and the adjacent cortical bone are well-integrated with each other, and the bottom regions of the cylinder have been eroded **(E)**. The scale bar represent 500 μm.

Figure 3

H-E staining on HAp/Col cylinder graft

Panels **A–C**, **D–F**, **G–I**, **J–L**, and **M–O** were obtained 3, 5, 7, 14, and 28 days after the HAp/Col grafting, respectively. Panels **A**, **D**, **G**, **J**, and **M** are low-magnification images of the HAP/Col cylinder. Panels **B**, **E**, **H**, **K**, and **N** and **C**, **F**, **I**, **L**, and **O** are histological images from the lateral and bottom regions, respectively. On day 3, the surface of the grafted HAp/Col cylinders look smooth, being surrounded by bone marrow tissue **(A–C)**. The dotted line indicates the boundary between the HAp/Col graft and the bone marrow **(C)**. On days 5 and 7, trabecular new bone is seen around the HAp/Col cylinder **(D, G)**. Trabecular new bones are continuous with the bottom surface of the cylinder **(F, I)**, whereas the new bones are discontinuous from the cylinder's lateral surface, with intervening stromal tissues (asterisks, **E, H)**. The dotted line indicates the boundary between the HAp/Col graft and the newly formed bone **(F, I)**. On day 14, in the lateral region, no continuity between the newly formed bone and the HAp/Col cylinder is seen yet due to intervening stromal tissue **(**asterisks, **J, K)**. Numerous multinucleated cells are localized on the lateral surface of the HAp/Col cylinder **(**arrows, **K)**, while the

bottom region has been fragmented into islands, with newly formed bone filling the spaces between them **(L)**. Note the multinucleated giant cells at the boundary between the HAp/Col graft and the new bone **(**arrows, **L)**. By day 28, the HAp/Col cylinder had collapsed, and newly formed bone had penetrated its interior in both the lateral and bottom regions **(M–O)**. The scale bars in **A, D, G, J,** and **M** represent 300 μm, while those in **B, C, E, F, H, I, K, L, N,** and **O** represent 100 μm.

Figure 4

Distribution of TRAP-positive osteoclasts

Panels **A–C**, **D–F**, **G–I**, **J–L**, and **M–O** were obtained 3, 5, 7, 14, and 28 days after the HAp/Col grafting respectively. Panels **A**, **D**, **G**, **J**, and **M** are low-magnification images of the HAP/Col cylinders. Panels **B**, **E**, **H**, **K**, and **N** and **C**, **F**, **I**, **L**, and **O** are histological images from the lateral and bottom regions, respectively. On day 3, TRAP-positive osteoclasts are nearly absent around the HAp/Col cylinder **(A–C)**. The dotted line indicates the boundary between the HAp/Col graft and the bone marrow **(C)**. On day 5, several TRAP-positive osteoclasts (red color, arrows) are localized along the lateral surface of the cylinder but not the bottom surface **(D–F)**. The dotted line indicates the boundary between the HAp/Col and newly formed bone **(F)**. The asterisks indicates stromal tissues **(E, H, K)**. By days 7 and 14, many TRAP-positive osteoclasts (arrows) have accumulated on the bumpy lateral surface of the HAp/Col cylinder **(G, H, J, K)**, allowing them to invade the cylinder's interior **(H, K)**. In contrast, in the bottom region, TRAP-positive osteoclasts (arrows) are seen in small numbers on day 7, but many were present on day 14 **(I, L)**. The dotted line indicates the boundary between the HAp/Col graft and the newly formed bone **(I)**. By day 28, TRAP-positive osteoclasts had completely invaded the HAp/Col cylinder **(M–O)**. The scale bars in **A, D, G, J,** and **M** represent 300 μm, while those in **B, C, E, F, H, I, K, L, N,** and **O** represent 100 μm.

Figure 5

Statistical analysis of the distribution of TRAP-positive osteoclasts

Panel **A** shows the number of TRAP-positive osteoclasts attached to the HAp/Col cylinder's surfaces, while panel **B** represents the total number of osteoclasts in the ROIs. The data are shown as the mean ± SE. Significant differences ($P < 0.05$) among means are represented using symbols: *, $P < 0.01$ and **, $P < 0.001$, for Dunnett's test results, and $^{\#\#}$, $P < 0.001$ for student's *t*-test results.

Figure 6

Distribution of PHOSPHO1-positive osteoblasts

Panels **A–C**, **D–F**, **G–I**, **J–L**, and **M–O** were obtained from 3, 5, 7, 14, and 28 days after the HAp/Col grafting, respectively. Panels **A**, **D**, **G**, **J**, and **M** are low-magnification images of the HAP/Col cylinders. Panels **B**, **E**, **H**, **K**, and **N** and **C**, **F**, **I**, **L**, and **O** are histological images from the lateral and bottom regions, respectively. On day 3, PHOSPHO1-positive osteoblasts are nearly absent from the surface of the HAp/Col cylinder **(A–C)**. The dotted line indicates the boundary between the HAp/Col graft and the bone marrow **(C)**. On days 5−7, PHOSPHO1-positive osteoblasts (brown color) can be seen in the new bone tissue around the HAp/Col cylinder **(D, G)**. In the lateral regions of the HAp/Col cylinder, PHOSPHO1-positive osteoblasts were seen in the new bone tissue at a distance from the lateral cylinder surface but not on the surface itself **(E, H**; note that no PHOSPHO1-positive cells are visible on the HAP/Col cylinder surface, as indicated by arrows**)**. However, PHOSPHO1-positive osteoblasts are located in the new bone tissue (asterisks) extending from the bottom surface of the cylinder **(F, I)**. The dotted line indicates the boundary between the HAp/Col graft and the newly formed bone **(F, I)**. On day 14, PHOSPHO1-positive osteoblasts can be seen on the trabecular bone at a distance from the lateral surface (arrows) of the HAp/Col cylinder but are still absent on the surface **(K)**, whereas lines of PHOSPHO1-positive osteoblasts (arrows) were noted on the newly formed bone (asterisk) in the bottom region **(L)**. By day 28, rows of PHOSPHO1-positive osteoblasts are observed throughout the HAp/Col cylinder **(M–O)**. The scale bars in **A, D, G, J,** and **M** represent 300 μm, while those in **B, C, E, F, H, I, K, L, N,** and **O** represent 100 μm.

Figure 7

Statistical analysis of the distribution of PHOSPHO1-positive osteoblasts

Panel **A** shows the number of TRAP-positive osteoclasts attached to the HAp/Col cylinder's surface, while panel **B** represents the total number of osteoclasts in the ROIs. The data are shown as the mean ± SE. Significant differences ($P < 0.05$) among means are represented using symbols: *, $P < 0.01$ and **, $P < 0.001$, for Dunnett's test results, and $^{\#\#}$, $P < 0.01$ and $^{\#}$, $P < 0.05$ for student's *t*-test results.

Figure 8

A schematic illustrating the findings of our study

After embedding an HAp/Col graft with laminated plates of horizontally orientated collagen fibers into the cavity defect in the tibia of a rat, osteoclasts accumulate in the region where the collagen fiber ends are exposed, while osteoblasts tend to adhere and induce bone formation in the regions where the collagen fibers run parallel to the bone tissue surface.